Available online at www.sciencedirect.com
SCIENCE DIRECT®
Journal of Catalysis 222 (2004) 293–306
JOURNAL OF CATALYSIS
www.elsevier.com/locate/jcat

Molecular structure and reactivity of vanadia-based catalysts for propane oxidative dehydrogenation studied by in situ Raman spectroscopy and catalytic activity measurements

Antonios Christodoulakis,[a] Maria Machli,[b] Angeliki A. Lemonidou,[b,*] and Soghomon Boghosian [a,*]

[a] *Department of Chemical Engineering, University of Patras and Institute of Chemical Engineering, Foundation of Research and Technology-Hellas (FORTH/ICE-HT), 26500 Patras, Greece*
[b] *Department of Chemical Engineering, Aristotle University of Thessaloniki and Chemical Process Engineering Research Institute, CERTH/CPERI, PO Box 1517, GR-54006 Thessaloniki, Greece*

Received 8 October 2003; accepted 13 October 2003

Abstract

The effect of support (ZrO_2 and TiO_2) and vanadia loading (1.2–10 wt%) on the molecular structure and the catalytic performance in propane oxidative dehydrogenation (ODH) were investigated using in situ Raman spectroscopy and catalytic activity measurements. In situ Raman spectra under oxidizing, reducing, and steady-state ODH reaction atmospheres were obtained for the studied catalysts. The main differences between the structure of VO_x entities in the two supporting materials derive from variations in the vanadia dispersion, which appears to be better in the case of the V_2O_5/TiO_2 compared to that of V_2O_5/ZrO_2 at the same VO_x density. In situ Raman spectra recorded in the presence of water vapor revealed that VO_x species are stable at high temperature while at low temperature the surface of the catalysts becomes hydrated. Significant perturbations of all kinds of V–O bonds were observed under reduction with propane and reaction conditions at 500 °C. The reactivity studies revealed that under the same reaction conditions oxidative dehydrogenation rates expressed per V atom are influenced by the type of the specific support and are functions of the VO_x density. The ability of vanadium to activate the C–H bond weakens with increasing VO_x density, whereby the number of V–O–M (M = support metal atom) bonds per V is reduced due to incorporation of vanadium in formation of V–O–V bridges. The combination of the results obtained from the in situ Raman spectra and the catalytic activity measurements points to a significance of V–O–support bonds in the kinetically significant reaction steps.

Keywords: Vanadia catalysts; Titania; Zirconia; Oxidative dehydrogenation; Propane; Raman spectroscopy

1. Introduction

Functionalization of light alkanes by selective oxidation, owing to the low cost and low environmental impact of these hydrocarbons, has attracted considerable research interest. The synthesis of C_2–C_4 alkenes from the corresponding alkanes in the presence of a catalyst and an oxidant (mainly oxygen) is one of the most challenging issues from a scientific and economic point of view [1]. The activation of the stable C–H bond of alkane at a low temperature while preserving the formed alkene from subsequent overoxidation is a prerequisite for a catalyst to be successful in the process. Among the catalysts that have been developed, vanadia catalysts are one of the more active and selective ones for the oxidative dehydrogenation of propane, as well as of butane and ethane [2–5].

Since vanadia-based catalysts are active at low temperatures where the reactions take place on the surface, the functionality of vanadia species on the catalyst surface is of great importance. Raman spectroscopy provides an important analytical tool for the identification of vanadia species present on the catalyst surface [6]. The molecular structures of such catalysts under dehydrated conditions evolve from isolated monovanadates and larger polyvanadates, where vanadium appears tetracoordinated, to bulk V_2O_5 crystals when vanadia loading exceeds the monolayer coverage of the support.

* Corresponding authors.
E-mail addresses: alemonidou@cheng.auth.gr (A.A. Lemonidou), bogosian@terpsi.iceht.forth.gr (S. Boghosian).

0021-9517/$ – see front matter
doi:10.1016/j.jcat.2003.10.007

Isolated monovanadates possess a terminal V=O bond and three V–O–M (M = metal atom of the oxide support) in a distorted tetrahedral configuration, O=V–(O–M)$_3$. Polymeric vanadates are formed by corner-sharing VO_4 tetrahedra, in which each of the V atoms has one terminal V=O bond, one, two, or three V–O–V bonds, and two, one, or zero V–O–M bonds [6,7]. The relative concentrations of the various surface vanadia species strongly depend on the specific metal oxide support, the surface vanadium density, and the calcination temperature of the sample.

The interaction of VO_x species with the supporting material affects the dispersion of these species on the surface. In general, basic metal oxide supports, such as MgO, strongly interact with VO_x, resulting in the formation of a mixed metal oxide rather than a stable surface vanadia overlayer [8,9]. Supports like alumina, zirconia, and titania allow good dispersion of surface vanadium oxide species [10–12]. Poorly dispersed V_2O_5 crystals on SiO_2, due to the weak interaction with the acidic V_2O_5 even at low surface coverage have been reported [13].

The acid-base character of the support modifies the acid-base properties of the support–vanadia overlayer interface and therefore determines the distribution of the surface species, the metal–oxygen bond strength, and the mean distance between the vanadium active centers [14–16], factors that appear to be of key importance for the catalytic performance of these materials.

Efforts aiming at the structural characterization of supported vanadium oxide on TiO_2 and ZrO_2 reveal that under dehydrated conditions and at low vanadia loadings vanadium exists as isolated monovanadates, whereas with increasing surface vanadia loading two- and three-dimensional polyvanadate layers are formed, which ultimately crystallize into bulk V_2O_5 crystals [17,18]. Moreover, for V_2O_5 catalysts supported on ZrO_2, formation of ZrV_2O_7 is reported at either high calcination temperatures and/or high VO_x surface densities (i.e., presence of crystalline V_2O_5) [19–21] or at low temperatures from interactions of surface-dispersed vanadia with the zirconia support [22].

Despite the great concern in the literature, a structure-reactivity/selectivity relationship for the oxidative dehydrogenation of propane over supported vanadium oxide catalysts still remains under debate [7,23–26]. Most of the characterization studies have been focused on the identification of molecular structures of supported vanadia catalysts either under ambient conditions or after pretreatment in O_2, H_2O, or hydrocarbon flow streams.

The present article focuses on the effect of the specific oxide support (ZrO_2, TiO_2) and the VO_x surface densities on the molecular structure and catalytic properties of surface vanadia species under propane oxidative dehydrogenation conditions at temperatures 300–550 °C. The in situ Raman spectra obtained under oxygen, propane, and reaction conditions provide useful structural information and their combination with the catalytic tests contributes to a better understanding of the behavior of these materials.

2. Experimental

2.1. Catalyst preparation

Supported vanadium oxide catalysts (1.2–10 wt% V_2O_5) were prepared by impregnation of anatase TiO_2 (Norton, SA = 50.8 m^2/g) and zirconia ZrO_2 (Norton, SA = 102.3 m^2/g). Prior to impregnation, the supports were crushed and sieved to a particle size of 100–180 μm. Vanadium was deposited on the supports by wet impregnation using aqueous NH_4VO_3 (99%, Merck) solution. Oxalic acid (99.5%, Riedel-de Haen) was added to the solution (NH_4VO_3/oxalic acid = 1/2 molar) to ensure dissolution of ammonium metavanadate precursor. After impregnation, the samples were dried overnight at 120 °C and calcined in synthetic air. The ZrO_2-supported samples were calcined at 600 °C for 6 h, while the ones supported on TiO_2 were calcined at 480 °C for 4 h. The chemical composition of the catalysts is presented in Table 1. The catalysts will be referred hereafter as xVTi or xVZr, where x is the nominal V_2O_5 loading of the catalyst.

Bulk ZrV_2O_7 was prepared by dry mixing of powdered ZrO_2 and V_2O_5 at equimolar quantities and calcination in air for 12 h at 650 °C, grinding, and subsequent calcination for another 12 h at 700 °C.

2.2. Catalyst characterization

The vanadium content of the catalysts was measured by inductively coupled plasma (ICP) technique using a Plasma 400 Perkin-Elmer apparatus. The surface area of the samples, using the multipoint BET analysis method, was measured by N_2 adsorption at −196 °C, using an Autosorb-1 Quantachrome flow apparatus. The samples were dehydrated in vacuum at 250 °C overnight, before surface area measurements. A Siemens D500 diffractometer was employed for the X-ray diffraction (XRD) patterns.

2.3. In situ Raman spectroscopy

Each catalyst was pressed into a self-supporting wafer (approximately 150 mg), which was mounted on a stainless-steel adjustable holder in the center of the in situ cell used for recording of the Raman spectra. The in situ cell is a kanthal-wound double-wall quartz-glass transparent tube furnace mounted on a xyz plate and possesses gas inlets and outlets as well as a thermocouple sheath in contact with the catalyst sample holder. The gases used were pure O_2 and 5% C_3H_8 balanced in He and were mixed by using thermal mass flowmeters in such a way that the reaction mixture contained O_2 and C_3H_8 in a 1:1 molar ratio (4.7% O_2, 4.7% C_3H_8, 90.6% He) at a total feed flow rate of 50 cm^3/min. In order to study the effect of H_2O vapors in the in situ Raman spectra, the dry gas was saturated in water vapor by feeding to a series of two flasks immersed in a thermostat at the appropriate temperature resulting in 8% H_2O vapor content.

The 488.0 or 514.5 nm lines of a Spectra Physics 164 Ar^+ laser were used for recording of the Raman spectra. The incident light was focused on the catalytic wafer by a cylindrical lens and operated at a power level of 40 mW at the sample. The scattered light was collected at 90° (horizontal scattering plane), analyzed with a 0.85 Spex 1403 double monochromator, and detected by a −20 °C cooled RCA photomultiplier equipped with EG&G photon counting electronics.

Prior to recording Raman spectra the samples were treated with flowing O_2 at 500 °C for 1 h in the Raman cell and spectra were then recorded in flowing O_2 at 500 °C. In situ spectra were obtained after 1 h of exposure of the studied catalyst in flowing C_3H_8/He and C_3H_8/O_2/He gases at a specified temperature. Before changing the gas atmosphere in the above sequence, the catalyst was cycled by being subjected to oxidation at 500 °C and the Raman spectra of the oxidized catalyst were reproduced.

2.4. Catalytic reaction

Catalytic experiments of the oxidative dehydrogenation of propane were conducted in a fixed-bed quartz reactor (i.d. 9 mm, length 300 mm) equipped with coaxial thermocouple for temperature monitoring. The catalyst loaded was mixed with equal amounts of quartz particles of the same size. Prior to the testing, the catalyst was treated in oxygen flow at 500 °C for 0.5 h. The composition of the reacting mixture used was $C_3H_8/O_2/He = 4.7/4.7/90.6$.

Two series of experiments were performed. In the first series, the performance of the samples was examined as a function of reaction temperature ranging from 300 up to 550 °C using the same catalyst weight ($W = 0.1$ g) and total flow rate ($F = 100$ cm^3/min). In the second series, the temperature was kept constant at 500 °C and the W/F ratio was varied from 0.002 to 0.3 g s cm^{-3}. Products were analyzed on line using a Varian 3400 chromatograph equipped with a TC Detector. Three columns in a series-bypass configuration were used in the analysis: a 20% BEEA–20% DC 200/500, a Porapak N-Chromosorb 106, and an MS 5A. The reaction products were mainly C_3H_6, CO_2, CO, and H_2O. Negligible amounts of oxygenates other than CO_x were detected at the reactor exit.

Carbon balance was closed up to 100 ± 1%. The selectivity of the products was calculated on a carbon basis. Under the conditions (temperature, flow) used in the catalytic tests, the conversion of propane in the empty reactor was lower than 2%, confirming that the extent of gas-phase reactions was negligible.

3. Results and discussion

3.1. Surface area and XRD

An overview of the basic characteristics of the prepared materials is compiled in Table 1. The catalysts supported on TiO_2 were calcined at a lower temperature (480 °C) compared to the catalysts supported on ZrO_2 (600 °C), because calcination at 600 °C was found to lead to the formation of a rutile phase, which was proved inactive for the ODH of propane [27]. A decrease of surface area is observed with the increase of vanadia loading for the TiO_2- and ZrO_2-based catalysts. The decrease is more severe with catalysts containing 10% vanadia, especially with that supported on ZrO_2 caused by the progressive formation of ZrV_2O_7 crystals, which block the pores of the support. Khodakov et al. [25] observed the same trend in surface areas for V_2O_5/ZrO_2catalysts calcined at 600 °C.

Table 1
Catalyst properties

Catalyst	V_2O_5 (wt%)	Calcination conditions	Surface area (m^2/g)	VO_x surface density, n_s (VO_x/nm^2)
1.5VZr	1.50	600 °C/6 h	73.4	1.3
2.5VZr	2.35	600 °C/6 h	73.6	2.1
5VZr	5.54	600 °C/6 h	65.7	5.5
10VZr	9.95	600 °C/6 h	29.7	22.0
1.2VTi	1.26	480 °C/4 h	46.8	1.8
2.5VTi	2.72	480 °C/4 h	44.5	4.0
5VTi	4.94	480 °C/4 h	43.0	7.6
10VTi	9.70	480 °C/4 h	29.1	22.0

The calculation of VO_x surface densities was based on the catalyst surface area. Densities from 1.3 up to 22.0 VO_x/nm^2 are obtained with the prepared catalysts. According to literature data, monolayer surface coverage determined from Raman spectroscopy measurements was found to be approximately 7–8VO_x/nm^2 [28].

XRD patterns of the catalysts are presented in Figs. 1 and 2. A monoclinic baddeleyite phase is detected in ZrO_2 samples. For the 1.5VZr and 2.5VZr samples vanadia seems to be finely dispersed (no other peaks except of the support), while characteristic peaks due to the mixed phase ZrV_2O_7 are observed in the pattern of 5VZr and 10VZr samples with increasing intensity. The formation of this mixed solid compound has been reported to be associated with high surface densities and/or high calcination temperatures of zirconia-

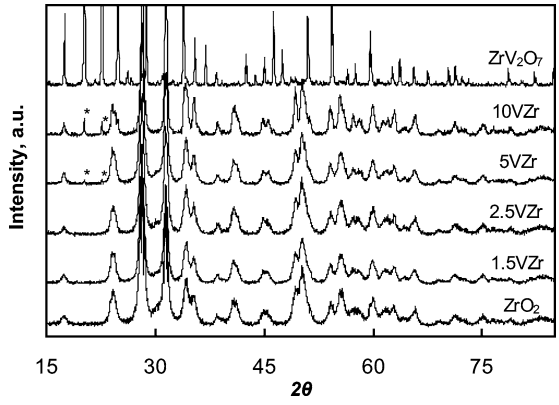

Fig. 1. X ray diffractograms of catalysts supported on zirconia (∗: ZrV_2O_7 peaks).

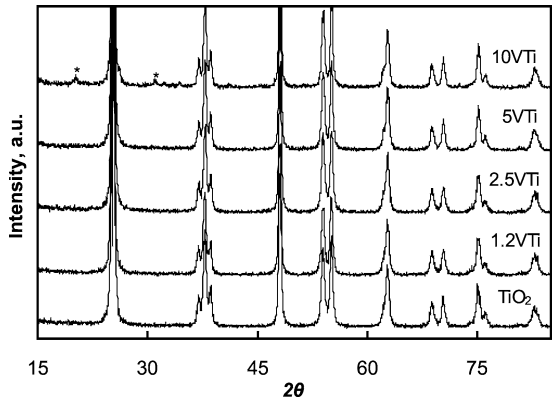

Fig. 2. X ray diffractograms of catalysts supported on titania (∗: V_2O_5 peaks).

supported vanadium oxide catalysts, and with the occurrence of ZrO_2 to its monoclinic phase [19–21]. Moreover, it may form from interactions of surface-dispersed vanadia with the zirconia support at low temperatures [22]. The diffractogram of the prepared pure ZrV_2O_7 phase is also included in Fig. 1. No other peaks apart from those corresponding to the mixed 1/1 V/Zr phase are observed.

The catalysts supported on TiO_2 with submonolayer VO_x densities (1.2, 2.5, and 5VTi) show only the peaks assigned to TiO_2 anatase (Fig. 2). The absence of V_2O_5 peaks is attributed to the very fine dispersion of V on the surface of the support. According to the literature, at low vanadia loading, V-oxide remains as a highly dispersed "monolayer" amorphous phase, while at higher loadings, crystalline V_2O_5 coexists with the "monolayer" phase [3]. Indeed, low intensity peaks of crystalline V_2O_5 are observed for the 10VTi catalyst, which has a VO_x density much higher than that of a monolayer.

3.2. *In situ Raman spectra of oxidized catalysts*

3.2.1. *V_2O_5/ZrO_2*

Raman spectra recorded for the catalyst samples containing 1.5–10 wt% V_2O_5, at 500 °C under oxidizing conditions, are presented in Fig. 3 which includes the Raman spectrum of the ZrO_2 support for comparison (spectrum 3a). It is evident that the strong band at ~ 620 cm^{-1} appearing in all spectra is due to zirconia substrate, which exists in monoclinic form.

Spectrum 3b, obtained for the 1.5VZr catalyst with a surface density (referred to hereinafter as n_s) of $1.3VO_x/nm^2$, exhibits (apart from bands due to the carrier) a well-defined band located at 1019 cm^{-1} and a weak very broad feature centered at 825 cm^{-1}. At low surface densities, dispersed vanadia occurs predominantly in the form of isolated monovanadates possessing one short V=O terminal bond and three anchoring V–O–support bonds, in a distorted tetrahedral VO_4 configuration, with C_{3v} symmetry. Thus, the 1019-cm^{-1} band can be assigned principally as due to V=O stretching mode of isolated monovanadates [7,17,19,23,29–32]. The presence, however, of the broad feature at 825 cm^{-1} is indicative of the presence of polyvanadates as well, since it is well known that a broad band at this location represents a wide set of configurations, arising from V–O stretching modes within polyvanadate structures, such as V–O–V modes [7,17,19,29,30,32].

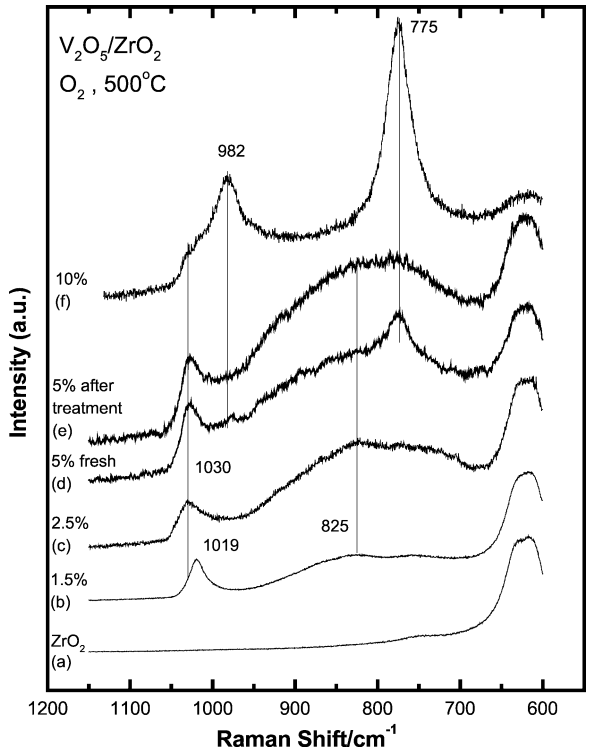

Fig. 3. In situ Raman spectra of ZrO_2-supported V_2O_5 catalysts taken under pure O_2 at 500 °C, for (a) unsupported ZrO_2; (b) 1.5 wt% V_2O_5/ZrO_2; (c) 2.5 wt% V_2O_5/ZrO_2; (d) 5 wt% V_2O_5/ZrO_2 (freshly calcined); (e) 5 wt% V_2O_5/ZrO_2 (after cycling, see text); (f) 10 wt% V_2O_5/ZrO_2. Laser wavelength, $\lambda_0 = 488.0$ nm; laser power, $w = 40$ mW; spectral slit width, ssw $= 7$ cm^{-1}; scan speed, ss $= 0.05$ cm^{-1} s^{-1}; time constant, $\tau = 9$ s.

With increasing surface density, one would expect that polyvanadates would occur predominantly on the catalyst surface. Indeed, as seen in spectrum 3c, the broad 700–950 cm^{-1} feature due to V–O modes along V–O–V chains grows in intensity relative to its intensity in spectrum 3b. In the same time the V=O mode is blue-shifted to 1030 cm^{-1} and possesses a low frequency shoulder at ~ 1020 cm^{-1}. Thus, the V=O mode of polyvanadates emerges at 1030 cm^{-1} and increasing amounts of such domains cause the observed shift from 1019 to 1030 cm^{-1}. The V=O mode of isolated monovanadates at 1019 cm^{-1} is obscured and can be seen as a low-frequency shoulder in spectrum 3c. It is evident, from Fig. 3c, that the relative population of polyvanadates is higher at the surface of the 2.5VZr compared to the 1.5VZr catalyst.

The peak mass of the 700–950 cm^{-1} very broad feature in Fig. 3c can be assigned to a distribution of V–O modes within polyvanadate domains, thus representing a broad set of configurations residing on the surface of the zirconia

support. Such polyvanadate species may contain one V=O bond, one, two, or three V–O–V bonds, and two, one, or zero V–O–*M* bonds per vanadium [7]. However, in order to obtain a polymeric chain, a significant portion of vanadium atoms should be involved in at least two V–O–V bridges. It is evident that such variations of the coordination around the vanadium atoms result in a wide distribution of bond orders among the V–O bonds of polyvanadates and account for the broadness of the 700–950 cm^{-1} feature.

The bond lengths and bond orders of terminal V=O, bridging V–O–V, and anchoring V–O–*M* bonds in monovanadate and polyvanadate species can be estimated from the following empirical formulas derived from an examination of a large number of model compounds [33]:

$$\nu = 21349\exp(-1.9176R), \tag{1}$$

$$\mathrm{BO} = \left[0.2912\ln(21349/\nu)\right]^{-5.1}, \tag{2}$$

where ν is the vibrational wavenumber (cm^{-1}), BO is the bond order, and R is the V–O bond length in Å. Eqs. (1) and (2) can be used in conjunction with observed Raman wavenumbers in order to check the consistency of proposed coordinations and band assignments with the constraint that the sum of the bond orders of V–O bonds involving a particular V(V) atom should be 5 valence units (vu).

Thus (checking the case of the isolated tetrahedral monomer O=V–(O–*M*)$_3$), the 1019-cm^{-1} band assigned to V=O terminal stretching corresponds to a bond order of 1.86 and the remaining 3.14 vu for the three V–O–*M* bonds corresponds to a bond order close to unity (1.05 vu) for each V–O–*M*. In turn, according to Eq. (2), the V–O-stretching frequency along the V–O–*M* bridge can be estimated at ~ 710 cm^{-1}. However, the presence of a Raman band in the low-frequency side of the broad 700–950 cm^{-1} feature cannot be evidenced in Fig. 3b with any degree of certainty, meaning that the V–O bond along the V–O–*M* of the isolated monomers, expected in the vicinity of 710 cm^{-1}, does not give rise to an observable Raman band.

In turn, we check the case of polyvanadate domains (Fig. 3c) containing a terminal V=O bond, two V–O–V bridging bonds, and one V–O–*M* bond. The 1030-cm^{-1} band assigned to V=O-terminal stretching, corresponds (using Eqs. (1) and (2)) to a bond order of 1.89; the 825-cm^{-1} band assigned to V–O–V corresponds to 1.32 vu and the remaining 0.54 vu is the V–O bond order along the V–O–*M* chain with an expected corresponding frequency (according to Eq. (2)) of ~ 440 cm^{-1}. Thus, it is evident that there are significant differences among V–O bond orders along V–O–support chains between isolated monovanadates and polyvanadate domains.

The in situ Raman spectrum of the fresh 5VZr catalyst with surface density of 5.5VO_x/nm^2 (obtained at 500 °C under flowing oxygen, after calcination) shown in Fig. 3d indicates that apart from amorphous surface vanadia, the ZrV_2O_7 crystalline mixed compound with characteristic bands at 775 and 975 cm^{-1} also exists on the catalyst surface [18,22,25]. XRD measurements (Fig. 1) also confirm the presence of the mixed ZrV_2O_7 crystalline phase.

The fresh 5VZr sample was subjected to sequential reduction (1 h in 5% C_3H_8/He) and oxidation (1 h in pure O_2) cycles at 500 °C and in situ spectra were obtained at 500 °C under flowing oxygen after each cycle. The bands attributed to the ZrV_2O_7 compound were gradually reduced in intensity and eventually almost disappeared after four reduction/oxidation cycles (Fig. 3e), while the peak mass attributed to polyvanadates was simultaneously growing in intensity. The absence of characteristic peaks due to the mixed phase was also observed in the XRD analysis of the 5VZr sample after 5 h under reaction conditions during the catalytic test (not shown). Further reduction/oxidation treatment of the sample did not alter the Raman characteristics. It is evident that zirconium vanadate occurring in the form of small domains below monolayer disperses easily under a reactive environment. Below, the surface structure of the "equilibrated" sample 5VZr will be presented and discussed. It is noteworthy, that in one case reported in the literature, after successive oxidation/reduction cycles of a V_2O_5/ZrO_2 catalyst with $n_s = 3.9VO_x/nm^2$, the V–O–V band was gradually shifted from 900 cm^{-1} (in the freshly calcined catalyst) to 770 cm^{-1} [7]. Such shifts have not been observed in the present study.

The spectrum of 5VZr catalyst (surface density 5.5VO_x/nm^2), shown in Fig. 3e, exhibits the characteristic features of polyvanadates; the Raman band due to V=O is at 1028 cm^{-1}, while the broad band assigned to V–O–V functionalities appears much more intense and its maximum is red-shifted, compared to the 2.5VZr catalyst with a lower VO_x density (Fig. 3c). This is in agreement with the expectation of a higher population of V–O–V bridges *per V atom* with increasing vanadia loading. Seen from another angle, as a result of the formation of polyvanadates with higher degree of polymerization, the number of V–O–*M* bridges (M = support metal atom) per V atom is progressively reduced from three (in the case of isolated monovanadates) to two, one, or even zero, as more V atoms get involved in V–O–V bridges with increasing fraction of larger polyvanadates. Elaborating the case of a unit possessing one V=O bond and three V–O–V-bridging bonds by using Eqs. (1) and (2) it turns out that the V–O bond order along the V–O–V bridges should be slightly above unity, giving rise to Raman bands in the low-frequency region of the broad 700–950 cm^{-1} feature, justifying the observed red shift of this band on going from spectrum 3c to 3e.

Furthermore, since the increasing fraction of polyvanadates induces an intensity enhancement in the 1028-cm^{-1} band on going from spectrum 3c to 3e, it is confirmed that the V=O-stretching mode of polyvanadates indeed occurs at 1028 cm^{-1}, obscuring the V=O-stretching modes of monovandates. The absence of the 994-cm^{-1} characteristic band of bulk V_2O_5 from the spectrum excludes the formation of crystalline V_2O_5.

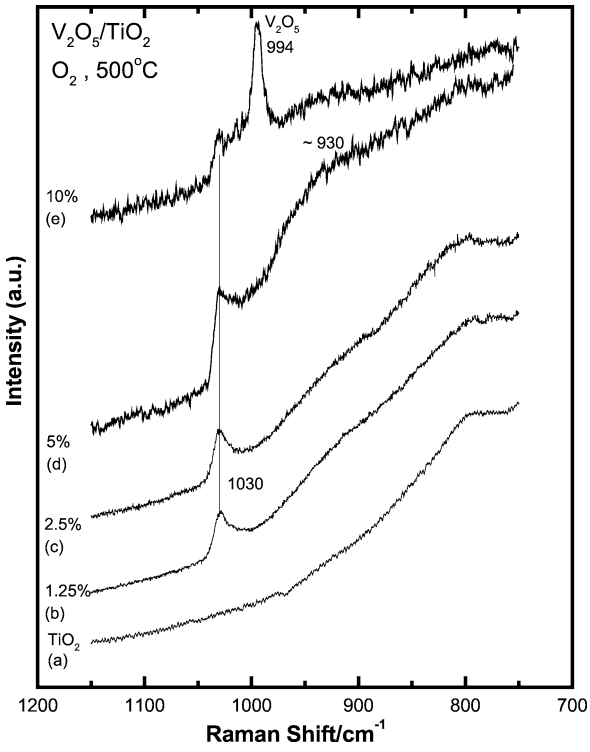

Fig. 4. In situ Raman spectra of TiO_2-supported V_2O_5 catalysts taken under pure O_2 at 500 °C, for (a) unsupported TiO_2; (b) 1.2 wt% V_2O_5/TiO_2; (c) 2.5 wt% V_2O_5/TiO_2; (d) 5 wt% V_2O_5/TiO_2; (e) 10 wt% V_2O_5/TiO_2. $\lambda_0 = 488.0$ nm; $w = 40$ mW; ssw $= 7$ cm^{-1}; ss $= 0.05$ cm^{-1} s^{-1}; $\tau = 9$ s.

The formation of the mixed ZrV_2O_7 compound is much more evident from the in situ Raman spectra obtained for the 10VZr catalyst with high surface density $22VO_x/nm^2$ (Fig. 3f), where the characteristic Raman bands at 775 and 982 cm^{-1} dominate in the spectrum. A remaining feature due to V=O at ~ 1030 cm^{-1} suggests the presence of amorphous surface vanadia along with the ZrV_2O_7 crystallites on the surface of the support. Contrary to the case of the 5VZr sample, no breakdown of ZrV_2O_7 was observed for 10VZr in reactive environment, indicating that large ZrV_2O_7 aggregates are stable above monolayer.

3.2.2. V_2O_5/TiO_2

In situ Raman spectra recorded for the 1.2–10 wt% V_2O_5/TiO_2 catalysts under O_2 flow at 500 °C are shown in Fig. 4. Due to strong scattering below 750 cm^{-1} arising from the titania support (Fig. 4a), spectra for the catalysts presented here are in the range from 750 to 1150 cm^{-1}.

The spectra obtained for the 1.2VTi and 2.5VTi catalysts (Fig. 4b and 4c), which have a surface density of 1.8 and $4VO_x/nm^2$, respectively, show that vanadia is dispersed in the form of isolated monovanadates as well as polyvanadate domains on the surface of the titania support. The well-defined band at 1030 cm^{-1} is assigned to the V=O stretching of dispersed vanadia species, whereas the weak broad band centered at ~ 920 cm^{-1} is due to V–O–V functionalities of polymeric species [34,35]. It is noteworthy that, although the 2.5VTi sample has a higher VO_x surface density compared to that of 2.5VZr, the intensity of the broad band due to polymeric vanadates is much lower, suggesting a lower population of V–O–V (polyvanadate) species and consequently a much better dispersion of vanadates (probably in the form of smaller domains) in the 2.5VTi sample. The same conclusion is drawn by exploiting the V–O–V band positions in the two sets of catalysts studied here (825 cm^{-1} for V_2O_5/ZrO_2 vs 920 cm^{-1} for V_2O_5/TiO_2) using Eqs. (1) and (2). Increasing the vanadium oxide content on the surface of the support (5VTi catalyst) results in a significant enhancement of the intensity of the broad band due to V–O–V functionalities (Fig. 4d). Worth noting is the absence of the characteristic 994-cm^{-1} band for crystalline V_2O_5, although the V surface density for this catalyst ($7.7VO_x/nm^2$) is very close to theoretical monolayer, $7–8VO_x/nm^2$ [28]. It is confirmed that a good dispersion is achieved with the formation of VO_x oligomers (i.e., dimers, trimers, etc.) instead of larger polyvanadate domains. This is in agreement with previous studies on VO_x/TiO_2 catalysts, reporting that vanadia is well dispersed on titania [17,18,36].

The characteristic 994-cm^{-1} band corresponds to crystalline V_2O_5 which is formed on the surface of 10VTi catalyst (Fig. 4e), with a surface density much higher than the theoretical monolayer. The weak 1030-cm^{-1} band indicates that a fraction of vanadia still remains dispersed on the catalyst surface. However, since the Raman scattering cross section is much more intense for the crystalline species, this observation should not be interpreted as indicating that the total amount of surface vanadia is not significant [37]. The V–O–V features of polyvanadates appear with reduced intensity relative to the 1030 cm^{-1} band. This is in agreement with Argyle et al. [38], who suggested that as the surface density increases, two- and three-dimensional polyvanadates form, which ultimately crystallize into bulk V_2O_5, with some evidence for residual monovanadate species.

3.2.3. *Effect of water vapor*

The presence of moisture, either in a reacting mixture or as a product in catalytic reactions, may affect the molecular structures of the surface metal oxide species and thereby the catalytic behavior. In fact, it has been known that H_2O(g) product retards the propane ODH over V_2O_5/ZrO_2 catalysts [39]. Therefore, it is of importance to investigate the effect of moisture on the dispersed surface species.

In situ Raman spectra were recorded for all catalysts studied under oxygen flow enriched with $\sim 8\%$ water vapors over a range of operating temperatures (500–150 °C). Representative results for the 5VZr catalyst are presented in Fig. 5, together with the Raman spectrum under pure oxygen conditions, at 500 °C.

It is clear that the presence of moisture does not cause any significant changes in the Raman spectrum obtained at 500 °C (Fig. 5b), except for a slight possible broadening of the 1028-cm^{-1} Raman band. This suggests that surface VO_x species are quite stable in the presence of water vapor at elevated temperatures. However, gradual lowering of the tem-

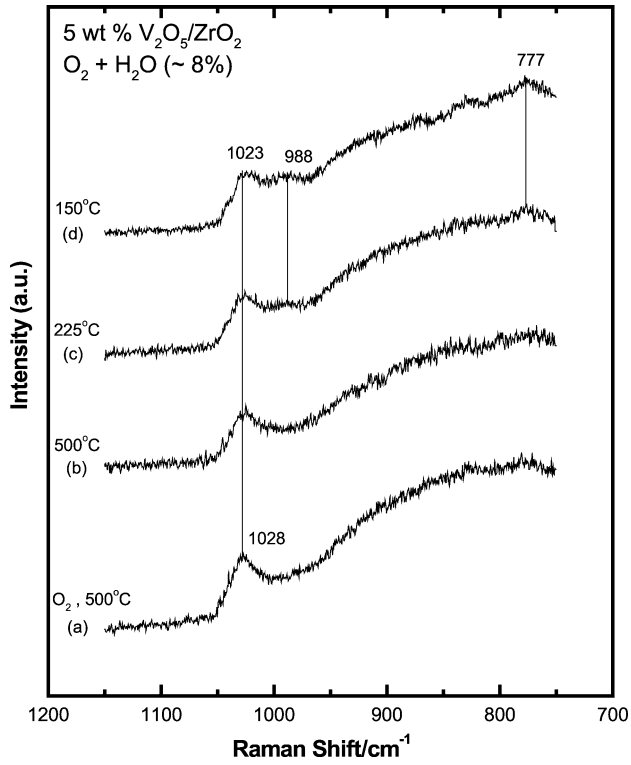

Fig. 5. In situ Raman spectra of 5 wt% V_2O_5/ZrO_2 catalyst taken under (a) O_2, 500 °C; (b) $O_2 + H_2O$, 500 °C; (c) $O_2 + H_2O$, 225 °C; (d) $O_2 + H_2O$, 150 °C. $\lambda_0 = 488.0$ nm; $w = 40$ mW; ssw $= 7$ cm^{-1}; speed, ss $= 0.05$ cm^{-1} s^{-1}; $\tau = 9$ s.

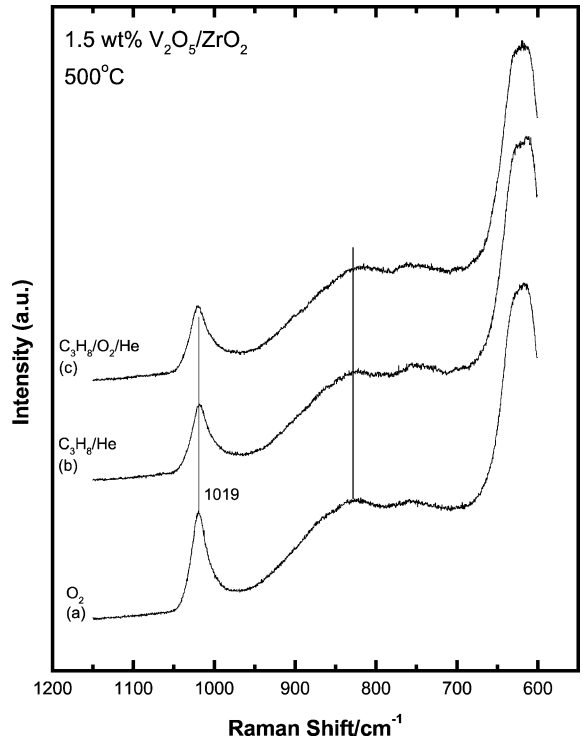

Fig. 6. In situ Raman spectra of 1.5 wt% V_2O_5/ZrO_2 catalyst taken at 500 °C under (a) O_2; (b) 5% C_3H_8/He; (c) 4.7% C_3H_8/4.7% O_2/He. $\lambda_0 = 488.0$ nm; $w = 40$ mW; ssw $= 7$ cm^{-1}; ss $= 0.05$ cm^{-1} s^{-1}; $\tau = 9$ s.

perature to 150 °C (Fig. 5c and 5d) results in a progressive red shift and broadening of the V=O band. On the contrary, the broad band due to the polyvanadate species does not seem to be as much affected by the presence of moisture. The ability of moisture to associate through hydrogen bonding to the oxygen involved in surface vanadia species at low operating temperatures has been well documented [40]. Thus, absorbed moisture interacts preferentially with surface vanadyl species, probably via hydrogen bonding on terminal V=O bonds, to an extent which is larger at lower temperatures. However, it remains questionable if possible perturbations of the broad bands due to the species possessing V–O–V bridges in the 820–920 cm^{-1} region would be detectable in the Raman spectra. Previously, changes in oxygen functionalities of surface polyvanadate species caused by the presence of H_2O/O_2 could be observed in oxygen-18 isotopic labeling experiments [40].

3.3. In situ Raman spectra under C_3H_8/He and C_3H_8/O_2/He gas atmospheres

3.3.1. V_2O_5/ZrO_2

The 1.5VZr, 2.5VZr, and 5VZr samples were examined in situ under reduction (5% C_3H_8/He) and ODH reaction conditions (4.7% C_3H_8, 4.7% O_2, 90.6% He) at 500 °C and the spectra are presented in Figs. 6–8. Prior to reduction and reaction experiments, the catalysts were oxidized in O_2 at

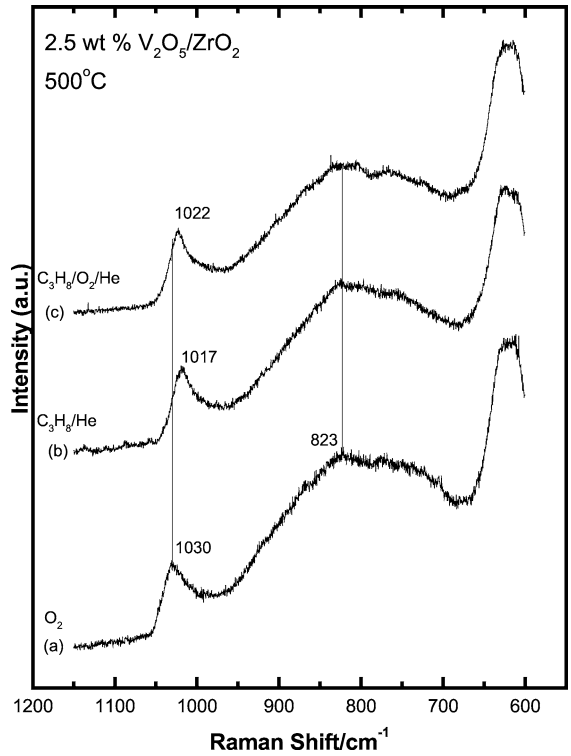

Fig. 7. In situ Raman spectra of 2.5 wt% V_2O_5/ZrO_2 catalyst taken at 500 °C under (a) O_2; (b) 5% C_3H_8/He; (c) 4.7% C_3H_8/4.7% O_2/He. $\lambda_0 = 488.0$ nm; $w = 40$ mW; ssw $= 7$ cm^{-1}; ss $= 0.05$ cm^{-1} s^{-1}; $\tau = 9$ s.

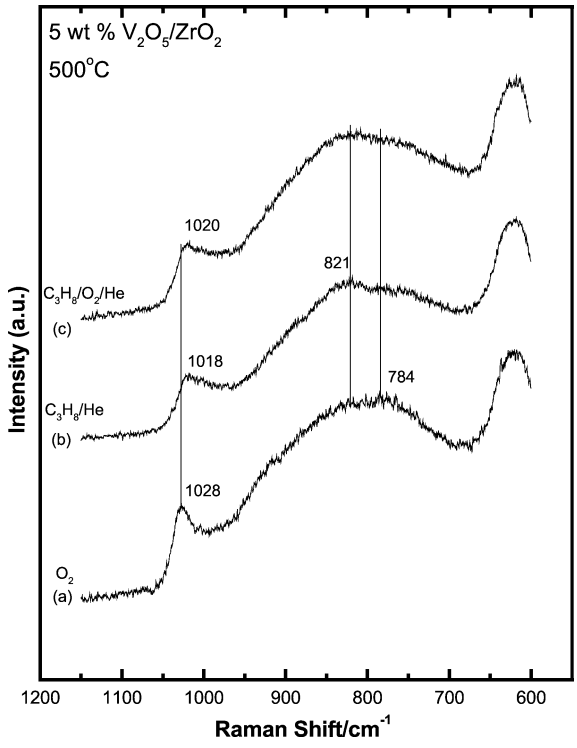

Fig. 8. In situ Raman spectra of 5 wt% V_2O_5/ZrO_2 catalyst taken at 500 °C under (a) O_2; (b) 5% C_3H_8/He; (c) 4.7% C_3H_8/4.7% O_2/He. $\lambda_0 = 488.0$ nm; $w = 40$ mW; ssw = 7 cm^{-1}; ss = 0.05 cm^{-1} s^{-1}; $\tau = 9$ s.

500 °C. Raman spectra were taken after 1 h exposure in the flowing gases. Each spectrum was normalized with respect to the band due to monoclinic ZrO_2, which at 500 °C appears centered at ~ 620 cm^{-1}.

The effects of exposing the 1.5VZr catalyst (with $n_s = 1.3 VO_x/nm^2$) to C_3H_8/He and C_3H_8/O_2/He atmospheres are shown in Fig. 6. The V=O band broadens slightly and looses some of its intensity. Moreover, the band due to V–O–V functionalities looses some of its intensity in a reducing or reaction environment. Such intensity loss can be accounted for by reduction of V^{5+} centers to lower oxidation states. By exploiting the intensities of the 825-cm^{-1} band due to V–O–V functionalities in spectra 6a–6c it turns out that a $\sim 4\%$ reduction of surface polyvanadates can be estimated in C_3H_8/He and C_3H_8/O_2/He atmospheres. The presence of O_2 (i.e., under steady-state reaction conditions, Fig. 6c) does not affect the extent of reduction.

Under a flow containing 5% C_3H_8 in He (i.e., under reducing conditions) the Raman spectrum (Fig. 7b) recorded for 2.5VZr (with $n_s = 2.1$ VO_x/nm^2) exhibits the V=O band red shifted from 1030 to 1017 cm^{-1}, while the polyvanadates band undergoes an intensity decrease. During propane ODH conditions (Fig. 7c) the V=O band appears in intermediate position, at 1022 cm^{-1}. Thus the presence of propane perturbs the V=O bond of the surface polyvanadate species to an extent which is affected by the presence of oxygen. The extent of reduction for polyvanadates, calculated by exploiting the intensities of the V–O–V bands in Fig. 7, is $\sim 4.5\%$ regardless of the presence of O_2. As vanadia loading increases further, the changes in the in situ Raman spectra under a C_3H_8/He and C_3H_8/O_2/He reaction mixture become more prominent. Thus in the Raman spectra of the 5VZr catalyst (with $n_s = 5.5$ VO_x/nm^2) under C_3H_8/He (Fig. 8b) the 1030 cm^{-1} V=O band appears weakened, broadened, and red shifted to 1018 cm^{-1} and the intensity loss of the V–O–V polyvanadates band is a lot more pronounced, when compared to, e.g., the intensity loss undergone by the corresponding band of the 2.5VZr sample (Fig. 7). During propane ODH conditions, the steady-state "snapshot" of 5VZr (Fig. 8c) exhibits features, which can be considered as intermediate of those seen in spectra 8a (O_2) and 8b (C_3H_8/He). The extent of reduction for polyvanadates, calculated based on the intensity loss of the V–O–V bands from the spectra in Fig. 8, is $\sim 24\%$ during reduction and $\sim 9\%$ during ODH reaction conditions. Thus, in agreement with Refs. [23,41], increasing vanadia loading causes a significant increase in the extent of reduction of polymerized surface vanadia in a reducing environment. The same effect but to a much smaller extent is also observed during steady-state oxidation conditions. The average oxidation state during catalytic operation depends on the balance between the reduction by the hydrocarbon molecule and the reoxidation by gas-phase molecular oxygen, and the reoxidation is reportedly faster than reduction [6].

The above estimations of the extent of reduction have been based on the assumption that the ~ 825-cm^{-1} band is representative of the polyvanadate species and that its intensity loss in environments containing propane is due to V^{5+} reduction. The trend in the estimated values is similar to previously reported results [23,41]. However, it has been postulated that apart from V^{5+} reduction, changes in coordination induced by chemisorbed gaseous reactants may perturb the V=O and V–O–V bonds in a way that could result in intensity loss of the corresponding bands [30].

There is a general consensus that ODH of propane over reducible oxides proceeds via Mars–van Krevelen redox-type reaction scheme, in which lattice oxygen atoms participate in the activation of C–H bonds in propane [3,39]. Moreover, it has been proposed that the activation of the C–H bond of alkanes involves the formation of an alkoxide as a reaction intermediate [42,43]. The coordination of such molecules to surface V sites would perturb the surface V–O bonds and thus would affect the spectral behavior of the catalysts under reaction conditions.

In addition, propane ODH turnovers involve one-electron reduction of two vanadium (V) cations, or a two—electron reduction of a single V^{5+} site, although the former case is more favorable, with respect to the activation energy required [44]. However, the present study cannot distinguish between the two possible scenarios. Further insight could be gained by methods, e.g., combined UV–vis/EPR [45], the use of which was beyond the scope of the present study.

It is noteworthy that reoxidation of the catalyst after each treatment cycle restores the reduced surface species to its

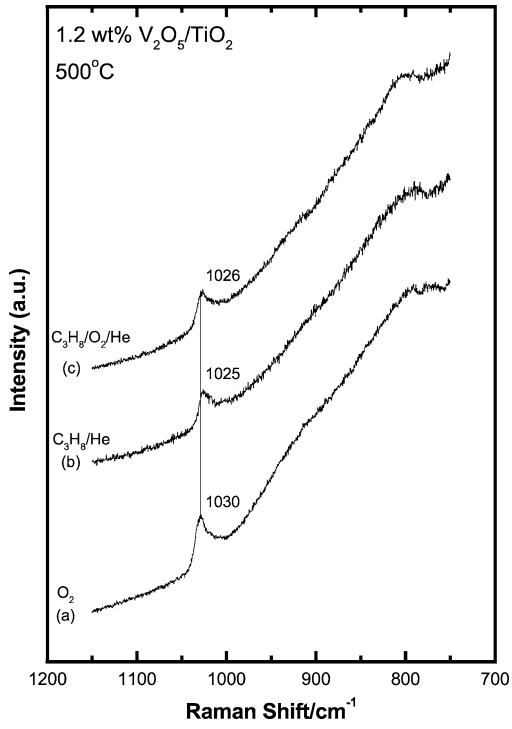

Fig. 9. In situ Raman spectra of 1.2 wt% V_2O_5/TiO_2 catalyst taken at 500 °C under (a) O_2; (b) 5% C_3H_8/He; (c) 4.7% C_3H_8/4.7% O_2/He. $\lambda_0 = 488.0$ nm; $w = 40$ mW; ssw $= 7$ cm^{-1}; ss $= 0.05$ cm^{-1} s^{-1}; $\tau = 9$ s.

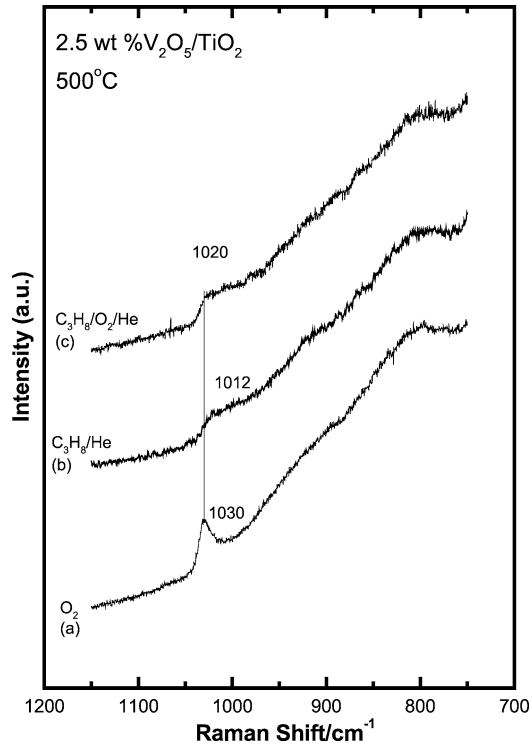

Fig. 10. In situ Raman spectra of 2.5 wt% V_2O_5/TiO_2 catalyst taken at 500 °C under (a) O_2; (b) 5% C_3H_8/He; (c) 4.7% C_3H_8/4.7% O_2/He. $\lambda_0 = 488.0$ nm; $w = 40$ mW; ssw $= 7$ cm^{-1}; ss $= 0.05$ cm^{-1} s^{-1}; $\tau = 9$ s.

fully oxidized form, reproducing the initial Raman spectrum (labeled as (a) in Figs. 6–8).

3.3.2. V_2O_5/TiO_2

Raman spectra under propane and propane ODH conditions were also recorded for all VTi catalysts but will be shown here only for 1.2VTi, 2.5VTi, and 5VTi, for brevity. Before reduction and reaction experiments, the catalysts were oxidized in O_2 at 500 °C for 1 h. Prior to recording each spectrum, catalyst samples were treated for at least 1 h with the corresponding gas feed. The spectra presented here have been normalized with respect to the 630-cm^{-1} titania (anatase) peak (not included in the scale of the figures).

The Raman spectra of the VTi catalysts studied under C_3H_8/He and C_3H_8/O_2/He conditions are compared with the corresponding spectra obtained under flowing O_2 and are shown in Figs. 9–11 for 1.2VTi, 2.5VTi, and 5VTi, respectively. An inspection of the spectra shown in Figs. 9–11 reveals that the spectra of 2.5VTi (Fig. 10) and 5VTi (Fig. 11) are affected to a larger extent compared to 1.2VTi (Fig. 9), indicating a higher extent of reduction and perturbation of the surface V^{5+} species. This is in line with the observed trends in the literature, according to which the extent of vanadium reduction increases with increasing surface density and that polyvandate species are characterized by higher reducibility compared to monovanadates [23,41]. Thus, the ~ 1030-cm^{-1} V=O band undergoes intensity loss, broadening, and red shift under C_3H_8/He, these effects being more moderate under steady-state reaction conditions

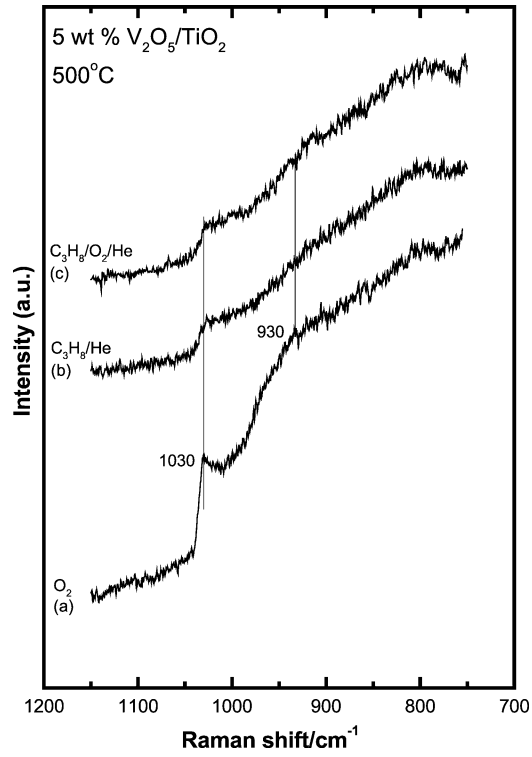

Fig. 11. In situ Raman spectra of 5 wt% V_2O_5/TiO_2 catalyst taken at 500 °C under (a) O_2; (b) 5% C_3H_8/He; (c) 4.7% C_3H_8/4.7% O_2/He. $\lambda_0 = 488.0$ nm; $w = 40$ mW; ssw $= 7$ cm^{-1}; ss $= 0.05$ cm^{-1} s^{-1}; $\tau = 9$ s.

(C_3H_8/O_2/He). As seen in Figs. 10 and 11, the effect is much more pronounced for 2.5VTi ($n_s = 4.0$ VO_x/nm^2) and 5VTi ($n_s = 7.6$ VO_x/nm^2) compared to 1.2VTi ($n_s = 1.8$ VO_x/nm^2). Furthermore, the 920- to 930-cm^{-1} band due to the V–O–V modes of polymeric vanadate species (which is very strong for the 5VTi sample under O_2; Fig. 11a) almost vanishes under reducing conditions (Fig. 11b). A partial restoration of the spectral features is observed under steady-state reaction conditions in all three samples, but still there appear significant perturbations of all kinds of observable V–O bonds. Although vanadium involved in polyvanadates appears very susceptible to reduction, it is the balance between the propane-induced reduction and the reoxidation, which determines the overall extent of reduction, under steady-state reaction conditions. Furthermore, as it was also observed in the case of zirconia-supported catalysts, vanadium V^{5+} centers coexist with vanadium in lower oxidation states under both gas atmospheres. Finally, it should be pointed out that although no reliable quantification of the extent of reduction can be made, it is evident that the V_2O_5/TiO_2 catalysts studied here exhibit much higher reducibility compared to the V_2O_5/ZrO_2 catalysts.

3.4. Catalytic results

The catalytic activity of each sample was measured over the range 300–550 °C using equimolar propane/oxygen feed at constant W/F ratio (0.06 g s cm^{-3}). The conversion and the selectivity toward propene were measured at regular temperature intervals. Characteristic values of propane conversion and product selectivities obtained at 400 °C are listed in Table 2. As shown in Table 2, when vanadia is supported on TiO_2, it results in much higher propane conversion than when supported on ZrO_2, in agreement with our previous results on the effect of support in propane oxidative dehydrogenation reactions [11]. Propene selectivities in both catalytic systems are rather low even at low degrees of propane conversion. Relatively low selectivities for vanadia catalysts supported on ZrO_2 and TiO_2 were also reported previously [11,46].

The variation of propane conversion as a function of temperature for all catalysts tested is shown in Fig. 12. The conversions increase with the temperature as was expected, but different behaviors are observed between the two sets of catalysts with varying V content. For the ZrO_2-supported samples, we observe significant variations in the degrees of conversion with 5VZr being the most active catalyst. The effect of V_2O_5 content at constant reaction temperature on propane conversion for the TiO_2-supported catalysts is different. The samples containing 5 and 10 wt% V_2O_5 exhibit the highest activity while the least active is the sample with the lowest V loading, 1.2 VTi.

Table 2
Catalytic results of propane ODH over V_2O_5/ZrO_2 and V_2O_5/TiO_2 catalysts at 400 °C

Catalyst	C_3H_8 conversion	Selectivity (%)		
	(%)	C_3H_6	CO	CO_2
1.5VZr	5.6	43.9	33.5	22.5
2.5VZr	7.1	35.9	42.5	21.6
5VZr	13.8	38.7	39.9	21.4
10VZr	3.3	51.2	37.7	11.1
1.2VTi	12.3	29.4	44.0	26.6
2.5VTi	21.2	19.9	61.5	18.6
5VTi	27.1	17.5	61.0	21.5
10VTi	27.6	13.6	68.1	18.3

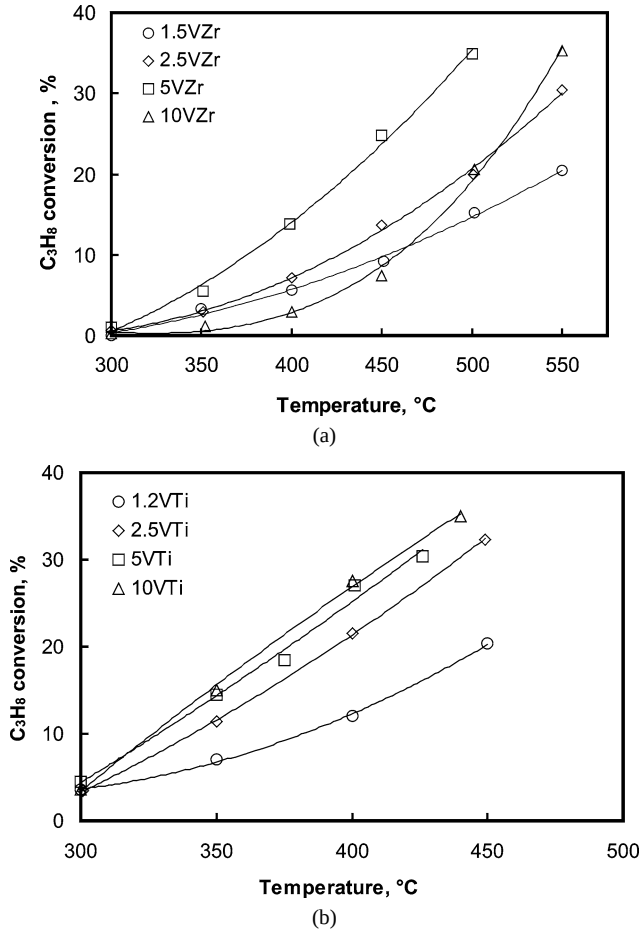

Fig. 12. Propane conversion as a function of temperature (a) ZrO_2-supported catalysts, (b) TiO_2-supported catalysts (W/F = 0.06 g s cm^{-3}, $C_3H_8/O_2 = 1/1$).

However, the above results cannot be used to gain an insight into the intrinsic activity of VO_x entities in propane ODH. Instead, differential reaction data (propane conversion less than 10%) obtained at two reaction temperatures, 300 and 500 °C, were used and the results are plotted in Fig. 13. The reaction rates were normalized by the number of V atoms (TOF, s^{-1}) to account for the different V_2O_5 content of the catalysts. Over the whole range of VO_x examined (1.3–22 VO_x/nm^2), rates over TiO_2-supported samples are higher (3 to 9 times) than that of the catalysts supported on ZrO_2 due the superior activity of VO_x domains on TiO_2 support. Fig. 13 shows that oxidative dehydrogenation rates depend not only on the support but also on VO_x

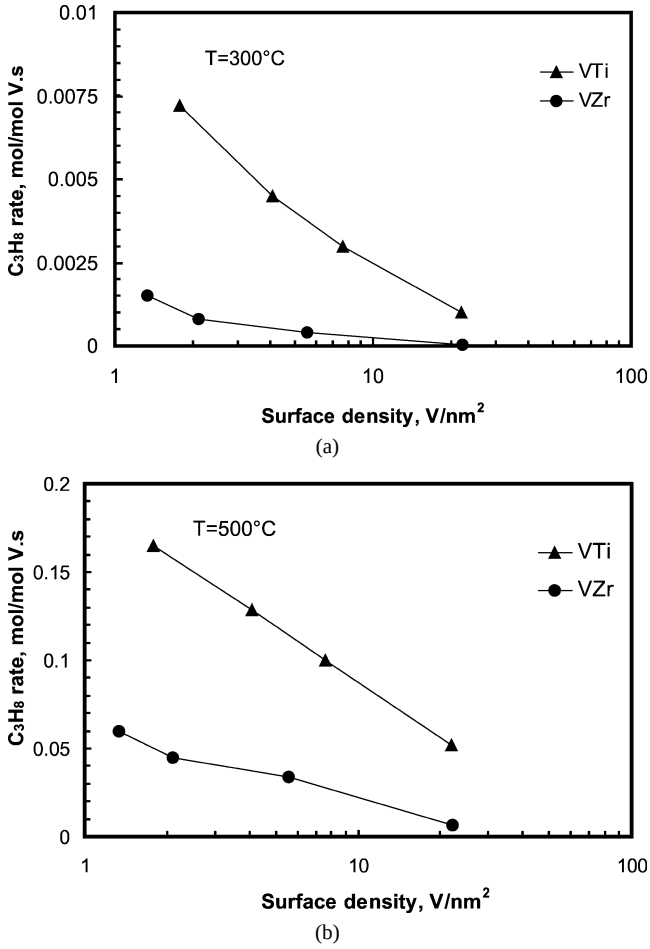

Fig. 13. Rate of C_3H_8 consumption as a function of VO_x surface density for $C_3H_8/O_2 = 1/1$. (a) 300 °C; (b) 500 °C. ▲, VTi; ●, VZr.

density, exhibiting a moderate decrease with increasing n_s. The decrease of TOF vs n_s is more pronounced for the TiO_2-supported catalysts. As shown in the previous section, VTi catalysts are much more reducible than VZr under steady-state reaction conditions. Therefore, it seems that the reactivity of the catalysts correlates with their reducibility [41]. It is thus confirmed that the local structure of VO_x active sites, which depends on the chemical identity of the support, significantly affects the ability to activate faster the C–H bond of the propane molecules. Wachs's group has also stressed the importance of the bridging V–O–*M* bonds for various supporting oxides in ethane ODH [41] and in selective oxidation of butane [47] and methanol [34].

Even though direct comparison of TOF values with literature data is not possible mainly due to differences in the catalytic samples, the ratio and the partial pressures of the reactants, present TOF values for the zirconia catalysts are in the same range with those reported by Gao et al. [23] and Khodakov et al. [25,26]. TOF values obtained with the TiO_2-supported catalysts are slightly higher than those reported in Ref. [26], while TOF values obtained with the ZrO_2-supported catalysts are slightly lower than those reported in Refs. [23,25,26].

The observed trends of TOF values vs n_s for surface coverages up to monolayer, showing a moderate decrease with increasing n_s, are quite interesting. It is seen that even at submonolayer surface coverages TOF values decrease especially for the TiO_2-supported samples. The rate decreases almost linearly with the VO_x, indicating that as the surface population of VO_x species increases, the sites for the activation of propane become less effective. Other authors reported that rates up to monolayer coverage are unaffected [23], initially increase and then decrease [25,26] with increasing VO_x density for ZrO_2-supported catalysts, and increase with increasing VO_x density for TiO_2-supported catalysts [26]. Variations observed for the trends of TOF values vs n_s will be readdressed in the next section.

For coverages above the monolayer the observed decrease in the rates over both supports could be attributed to less exposed V sites present in crystalline phases (ZrV_2O_7 or V_2O_5) and covering of the active surface sites by the crystallites in agreement with literature data for, e.g., V_2O_5/ZrO_2 catalysts with V loading higher than a monolayer [25].

The bond order of terminal V=O bonds was found to be independent on the specific metal oxide support, judging from the position of the ν(V=O), which is the same for VTi and VZr catalysts. However, the estimated TOF values over the samples with similar VO_x surface densities on TiO_2 and ZrO_2 vary considerably. Thus, the role of this bond on the activation of the propane molecule is not of critical importance [23,28,47,48]. Wachs et al. [47] based on in situ Raman studies with oxygen-18 labeling of the terminal V=O bond during butane oxidation showed that the exchange time of this band was ~ 20 times longer than the characteristic reaction time (1/TOF), suggesting that this bond is too stable to be involved in the rate-determining step of the reaction.

On the contrary, the observation of higher rates of propane conversion (per V atom) for the catalyst samples possessing a relatively higher population of V–O–support bonds points to a significance of these bonds toward the C–H activation. Moreover, the enhanced catalytic performance, when switching from ZrO_2 to TiO_2 support, underlines the crucial role of the supporting material. Consequently, the nature of the V–O–*M*-anchoring bonds appears as the determinant factor for the catalytic behavior of the catalysts studied here.

In order to examine the effect of V content on propene selectivity, runs were conducted at 500 °C using various W/F ratios to attain different degrees of propane conversion. Since selectivity is mainly determined by conversion, the obtained selectivity values were plotted versus conversion (Fig. 14). The performance of the two catalytic systems examined in terms of selectivity has many similarities. The catalytic samples supported on titania and zirconia with VO_x coverages equal or lower than a monolayer exhibit almost the same selectivity over the whole range of the conversions attained. The two samples with the highest V loading (10 wt%) exhibit lower selectivities. It seems that the presence of crystalline phases, ZrV_2O_7 for catalysts supported

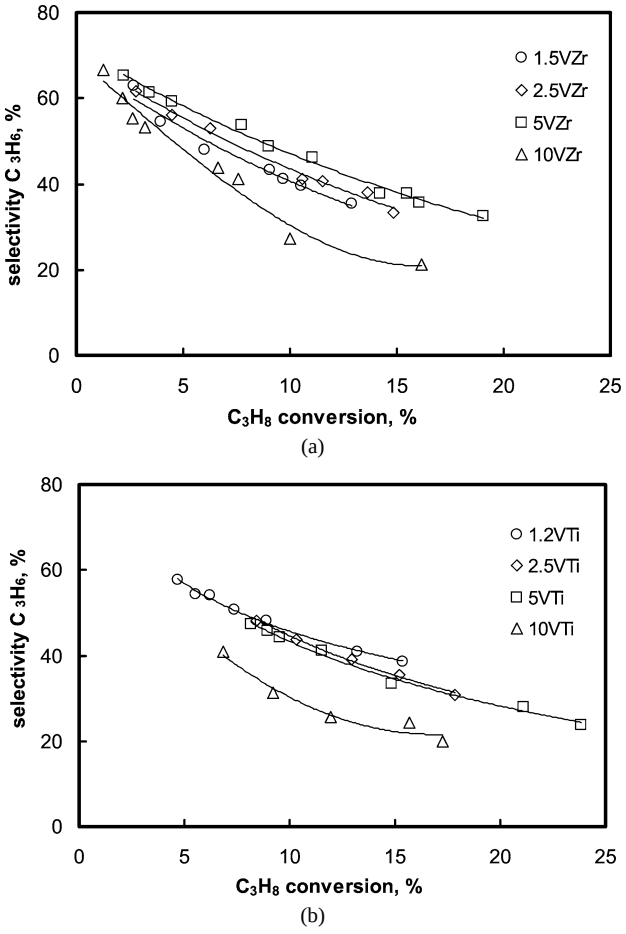

Fig. 14. Selectivity as a function of conversion (a) ZrO_2-supported catalysts, (b) TiO_2-supported catalysts ($T = 500\,^{\circ}C$, $C_3H_8/O_2 = 1/1$).

on ZrO_2 and V_2O_5 for catalysts supported on TiO_2, apart from decreasing the rates of the reaction, facilitate also deep oxidation of propane and/or propene. However, it should be noted that the ZrV_2O_7 phase is not totally unselective as it was reported [25]. Indeed, when pure ZrV_2O_7 was tested under propane ODH conditions it was found that at low propane conversion (5%) the selectivity to propene was 72% almost the same with the one observed with the other VZr samples. It appears that the primary steps of ODH are not influenced by the mixed phase. However, at higher conversion where secondary reactions of propene are of significance, the presence of crystalline phases is detrimental. It is probable that adsorption of propene molecules on these sites is very strong, favoring their oxidation to CO_x.

From the selectivity/conversion plots we imply that up to monolayer coverage the VO_x density and the support nature do not seem to differentiate the reaction sequence for the TiO_2- and ZrO_2-supported catalysts.

3.5. Structure-activity relationships

Trends reported in the literature concerning the dependence of TOF on vanadium surface density for the ODH of propane over supported metal oxide catalysts are far by universal. Selected options of behavior *for catalysts with coverage below monolayer* include—but are not restricted to—not significant variation in TOF for V_2O_5/ZrO_2 [23] and V_2O_5/Al_2O_3 catalysts [14], constant TOF as a function of surface vanadia coverage for propane oxidation over V_2O_5/Nb_2O_5 catalysts [49], initial increase (for small n_s values) and then decrease for V_2O_5/ZrO_2 catalysts [25], and monotonic increase for V_2O_5/M_xO_y (M = Al, Hf, Si, Ti, Zr) catalysts [26]. A moderate decrease in TOF values as a function of vanadium surface density has been observed in the present study for V_2O_5/M_xO_y (M = Zr, Ti) catalysts samples with coverage below monolayer. Gao et al. [23] addressed this controversy by focusing on the case of V_2O_5/ZrO_2 catalysts and numbered certain factors, which may contribute to the above differences. They pointed out that the sample preparation method (different in Lehigh and Berkeley) as well as differences in the ZrO_2 phases present and in calcination temperature could account partially for the observed differences. However, there are more points calling attention. Gao et al. [23] were the first to study the effect of C_3H_8/O_2 ratio on a number of factors including the TOF vs n_s trends by varying the C_3/O_2 ratio from 0.1 to 3. Khodakov et al. [26] used a feed gas with C_3/O_2 ratio equal to 8 and although they see a monotonic increase of TOF vs n_s for V_2O_5/M_xO_y (M = Al, Hf, Si, Ti), for the V_2O_5/ZrO_2 case they observe an initial increase followed by a decrease, which resembles the TOF vs n_s trend shown by Gao et al. for a feed gas with C_3/O_2 ratio equal to 3. Furthermore, the observed moderate decrease of TOF vs n_s for the V_2O_5/ZrO_2 case in the present work, where the feed gas has a C_3/O_2 ratio equal to 1, is in line with the moderate decrease shown by Gao et al. [23] for a feed gas with C_3/O_2 ratio equal to 0.5. In order to contribute more essentially to this discussion we would like to point out certain aspects related to molecular structure of surface vanadia species that cannot be disregarded. For the dispersed polyvanadate species at the surface of ZrO_2 in dehydrated conditions, Khodakov et al. [25] report a V=O bond at 1025 cm^{-1} and a strong broad V–O–V bond centered at 860 cm^{-1}, Gao et al. [23] report a V=O bond at 1020 cm^{-1} and a strong broad V–O–V bond centered at 935 cm^{-1}, whereas in the present study we observe a V=O bond at 1030 cm^{-1} and a strong broad V–O–V bond centered at 825 cm^{-1}. It is evident that variations in the molecular structure (reflected by the differences in the Raman wavenumbers) may account for the observed differences in TOF trends. Table 3 compiles certain selected properties of the catalysts discussed above. Raman "snapshots" of operating catalysts with simultaneous activity measurements ("operando spectroscopy" [50–52]) may shed more light on the above discussion.

The ability of V to activate the C–H bond appears to weaken with increasing vanadia loading. Formation of polyvanadate domains in V_2O_5/ZrO_2 and V_2O_5/TiO_2 catalysts, where *the number of* V–O–*M bonds per V is lowered* with increasing VO_x density due to incorporation of vanadium in V–O–V bridges, is accompanied with a moderate reduction

Table 3
Observed vibrational V–O bond wavenumbers, textural properties, and catalytic behavior in ODH of propane for V_2O_5/ZrO_2 catalysts

	Khodakov et al. [25]	Khodakov et al. [26]	Gao et al. [23]	This work
Monovanadate, V=O (cm^{-1})	1025[a]	1028	1034	1019
Polyvanadate, V=O (cm^{-1})	1025[a]		1020	1030
Polyvanadate, V–O–V (cm^{-1})	860, br[b]		935, br[b]	825, br[b]
Polyvanadate, V=O and V–O–V (cm^{-1})		700–980		
Calcination temperature (°C)	400, 500, 600	500	450	600
Zirconia phases	> 50% Tetragonal, Monoclinic	Mainly Tetragonal	Monoclinic[c]	Monoclinic
SA_{BET} (m^2/g)	180–340[d]	144–170	⩽ 34	30–73
n_s, VO_x/nm^2	0.4–100	0.9–6.2	Up to 8.1	1.3–22.0
Major crystalline phases containing V, just above monolayer	ZrV_2O_7 (and small V_2O_5 clusters)[e]	Traces of ZrV_2O_7 and V_2O_5	V_2O_5	ZrV_2O_7
TOF vs n_s (below monolayer)	Initial increase, then decrease	Increase (see text: initial increase, then decrease)	Not significant variation (see text: moderate decrease for $C_3H_8/O_2 = 0.5$)	Moderate decrease
C_3H_8/O_2	8	8	0.1, 0.5, 3	1

[a] Assigned to V=O without specifying if band is due to monovanadate or polyvanadate [25].
[b] br, broad.
[c] Mentioned as monoclinic under Experimental section and tetragonal under Discussion [23].
[d] After drying at 120 °C. SA_{BET} varies between 25 and 250 m^2/g depending on loading and calcination temperature [25].
[e] For calcination temperature 600 °C [25].

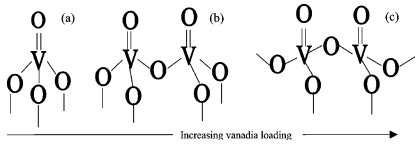

Fig. 15. Schematic drawing of surface vanadia species with increasing vanadia loading (a) isolated monovanadates; (b) vanadate dimers; (c) polyvanadates.

of their activities. Fig. 15 depicts molecular models of supported VO_x species, in which it can be seen that the number of V–O–*M* bonds per vanadium atom is reduced with increasing loading, as more V atoms get involved in formation of V–O–V bridges. This observation points to a significance of the V–O–*M* (*M* = Zr, Ti) centers for the catalytic activity. Moreover, the catalytic activity appears to strongly depend on the support material, i.e., on the *nature* of the V–O–*M* bonds. This becomes evident when comparing catalysts with equal vanadium surface densities but with different supports, thus raising the significance of V–O–*M* centers even further.

4. Conclusions

Vanadia catalysts with densities from 1.3 to 22 VO_x/nm^2 supported on titania and zirconia exhibit interesting catalytic properties in propane oxidative dehydrogenation. The in situ Raman studies provided useful information about the structure of VO_x species on the catalyst surface under various atmospheres. The fully oxidized surface at 500 °C exhibits two types of VO_x species: monovanadates and polyvanadates at various compositions depending on the density of VO_x. Polyvanadates (along with monovanadates) are formed at the ZrO_2 surface even at low VO_x densities (1.3 VO_x/nm^2) while at the TiO_2 surface monovanadates prevail at low VO_x densities. Furthermore, the polyvanadates formed on TiO_2 seem to consist of small chains of V–O–V. For VO_x densities over monolayer (> 8 VO_x/nm^2) crystalline V_2O_5 and ZrV_2O_7 are formed on TiO_2 and ZrO_2, respectively. The presence of water vapors does not seem to affect the structure of VO_x domains at 500 °C in oxidizing atmosphere while at low temperature (< 225 °C) the presence of water distorts the surface vanadia species. The changes in Raman spectra (red-shift of V=O band accompanied by reduced intensities of both monovanadate and polyvanadate bands) obtained under propane flow (reducing conditions) were ascribed to the reduction of V^{5+} centers to lower oxidation and/or to perturbations of V–O bonds caused by neighboring propane molecules. Significantly higher degrees of reduction of VO_x species were observed with the TiO_2- than with the ZrO_2-supported catalysts. The reactivity studies revealed that under the same reaction conditions oxidative dehydrogenation rates expressed per V atom are functions of the specific support and the VO_x density. VO_x species supported on TiO_2 are more active than those supported on ZrO_2, showing that the role of V–O–support bonds in the C–H bond activation, the kinetically relevant step, is determinant. The ability of V to activate the C–H bond appears to weaken with increasing vanadia loading (which results in an increase in V surface density) for both cases of support materials studied (ZrO_2 and TiO_2). Formation of polyvanadate domains in catalysts with high vanadia loadings, where *the number of V–O–M bonds per V is lowered* due to incorporation of vanadium in V–O–V bridges, is accompanied with moderate reduction of their activities.

Acknowledgments

The financial support of the Research Committee, University of Patras (C. Caratheodory grant for basic research), and of the EPEAEK/HERAKLEITOS programme of the Greek Ministry of Education is acknowledged by A. Christodoulakis and S. Boghosian. The financial support of GSRT (PENED2002) is gratefully acknowledged by M. Machli and A.A. Lemonidou.

References

[1] G. Centi, F. Cavani, F. Trifiro, Selective Oxidation by Heterogeneous Catalysis, Kluwer Academic/Plenum, New York, 2001.
[2] T. Blasco, J.M. Lopez Nieto, Appl. Catal. A 157 (1997) 117.
[3] E.A. Mamedov, V. Cortes Corberan, Appl. Catal. A 127 (1995) 1.
[4] M.A. Banares, Catal. Today 51 (1999) 319.
[5] H.H. Kung, Adv. Catal. 40 (1994) 1.
[6] M.A. Banares, I.E. Wachs, J. Raman Spectrosc. 33 (2002) 359.
[7] S.C. Su, A.T. Bell, J. Phys. Chem. B 102 (1998) 7000.
[8] H.H. Kung, M.C. Kung, Appl. Catal. A 157 (1997) 105.
[9] D. Siew Hiew Sam, V. Soenen, J.C. Volta, J. Catal. 123 (1990) 417.
[10] G.C. Bond, S. Flamerz Tahir, Appl. Catal. 71 (1991) 1.
[11] A.A. Lemonidou, L. Nalbandian, I.A. Vasalos, Catal. Today 61 (2000) 333.
[12] F. Arena, F. Frusteri, A. Parmaliana, Appl. Catal. A 176 (1999) 189.
[13] J. Haber, A. Kozlowska, R. Kozlowski, J. Catal. 102 (1986) 52.
[14] J.G. Eon, R. Olier, J.C. Volta, J. Catal. 145 (1994) 318.
[15] T. Blasco, J.M. Lopez Nieto, A. Dejoz, M.I. Vazquez, J. Catal. 157 (1995) 271.
[16] B. Grzybowska-Świerkosz, Top. Catal. 11/12 (2000) 23.
[17] G.T. Went, S.T. Oyama, A.T. Bell, J. Phys. Chem. 94 (1990) 4240.
[18] B. Olthof, A. Khodakov, A.T. Bell, E. Iglesia, J. Phys. Chem. B 104 (2000) 1516.
[19] F. Roozeboom, M.C. Mittelmeijer-Hazeleger, J.A. Moulljn, J. Medema, V.H.J. de Beer, P.J. Gellings, J. Phys. Chem. 84 (1980) 2783.
[20] J.R. Sohn, S.G. Cho, Y.I. Pae, S. Hayashi, J. Catal. 159 (1996) 170.
[21] J.L. Male, H.G. Niessen, A.T. Bell, T. Don Tilley, J. Catal. 194 (2000) 431.
[22] C.L. Pieck, M.A. Banares, M.A. Vicente, J.L.G. Fierro, Chem. Mater. 13 (2001) 1174.
[23] X. Gao, J.-M. Jehng, I.E. Wachs, J. Catal. 209 (2002) 43.
[24] G. Garcia Cortez, M.A. Banares, J. Catal. 209 (2002) 197.
[25] A. Khodakov, J. Yang , S. Su, E. Iglesia, A.T. Bell, J. Catal. 177 (1998) 343.
[26] A. Khodakov, B. Olthof, A.T. Bell, E. Iglesia, J. Catal. 181 (1999) 205.
[27] M. Machli, E. Heracleous, A.A. Lemonidou, Appl. Catal. A 236 (2002) 23.
[28] I.E. Wachs, B.M. Weckhuysen, Appl. Catal. A 157 (1997) 67.
[29] I.E. Wachs, Catal. Today 27 (1996) 437.
[30] L.J. Burcham, G. Deo, X. Gao, I.E. Wachs, Top. Catal. 11/12 (2000) 85.
[31] I. Giakoumelou, Ch. Fountzoula, Ch. Kordulis, S. Boghosian, Catal. Today 73 (2002) 255.
[32] G. Busca, J. Raman Spectrosc. 33 (2002) 348.
[33] F.D. Hardcastle, I.E. Wachs, J. Phys. Chem. 95 (1991) 5031.
[34] G. Deo, I.E. Wachs, J. Catal. 146 (1994) 335.
[35] G.T. Went, L.J. Leu, R. Rosin, A.T. Bell, J. Catal. 134 (1992) 479.
[36] V.I. Parvulescu, S. Boghosian, V. Parvulescu, S.M. Jung, P. Grange, J. Catal. 217 (2003) 172.
[37] S. Xie, E. Iglesia, A.T. Bell, Langmuir 16 (2000) 7162.
[38] M.D. Argyle, K. Chen, A.T. Bell, E. Iglesia, J. Catal. 208 (2002) 139.
[39] K. Chen, A. Khodakov, J. Yang, A.T. Bell, E. Iglesia, J. Catal. 186 (1999) 325.
[40] J.M. Jehng, G. Deo, B.M. Weckhuysen, I.E. Wachs, J. Mol. Catal. A 110 (1996) 41.
[41] M.A. Banares, M.V. Martinez-Huerta, X. Gao, J.L.G. Fierro, I.E. Wachs, Catal. Today 61 (2000) 295.
[42] G. Busca, E. Finocchio, V. Lorenzelli, G. Ramis, M. Baldi, Catal. Today 49 (1999) 453.
[43] K. Chen, A.T. Bell, E. Iglesia, J. Phys. Chem. B 1041 (2000) 1292.
[44] K. Chen, A.T. Bell, E. Iglesia, J. Catal. 209 (2002) 35.
[45] A. Bruckner, Chem. Commun. (2001) 2122.
[46] R. Grabowski, B. Grzybowska, K. Samson, J. Słoczyński, J. Stoch, K. Wcisło, Appl. Catal. A 125 (1995) 129.
[47] I.E. Wachs, J.M. Jehng, G. Deo, B.M. Weckhuysen, V.V. Guiliants, J.B. Benziger, Catal. Today 32 (1996) 47.
[48] B.M. Weckhuysen, D.E. Keller, Catal. Today 78 (2003) 25.
[49] T.C. Watling, G. Deo, K. Seshan, I.E. Wachs, J.A. Lercher, Catal. Today 28 (1996) 139.
[50] B.M. Weckhuysen, Chem. Commun. (2002) 97.
[51] G. Garcia Cortez, M.A. Banares, J. Catal. 209 (2002) 197.
[52] M.O. Guerrero-Perez, M.A. Banares, Chem. Commun. (2002) 1292.